Contribution from the Department of Chemistry,
McMaster University, Hamilton, Ontario, L9H 3R9, Canada

Lewis Acid–Base Properties of Iodine(VII) Dioxide Trifluoride

R. J. GILLESPIE* and J. P. KRASZNAI

Received June 7, 1977 AIC60463N

The ^{19}F NMR and laser Raman spectra of the adducts of IO_2F_3 with AsF_5, SbF_5, NbF_5, TaF_5, IF_5, and IOF_3 have been measured. The spectra show that the adducts are oxygen-bridged polymers of the type $(IO_2F_4{\cdot}MF_4)_n$ and $(IO_2F_4{\cdot}IOF_2)_n$, respectively. The reaction between KIO_4 and IF_5 has been reinvestigated by ^{19}F NMR and Raman spectroscopy and it has been shown that the previously obtained solid of composition $KIO_4{\cdot}IF_5$ is a mixture of KIO_2F_4 and IO_2F. By the same reaction we have also made the adduct $KIO_2F_4{\cdot}2IF_5$ and from this pure KIO_2F_4. The $IO_2F_4^-$ ion in KIO_2F_4 has been shown, by ^{19}F NMR and Raman spectroscopy, to have the trans (D_{4h})structure. In IF_5 solution *trans*-$IO_2F_4^-$ isomerizes to a mixture of the cis and trans isomers.

Introduction.

In a previous paper,[1] we have shown that iodine dioxide trifluoride has the cyclic trimeric structure shown in Figure 1. In forming this trimer the IO_2F_3 monomer is displaying both donor and acceptor properties; each IO_2F_3 monomeric unit in the trimer uses one of its oxygen atoms to form a donor bond with its neighboring iodine and at the same time the iodine accepts an electron pair from the oxygen of a neighboring IO_2F_3. The present paper is concerned with the general donor and acceptor or Lewis acid–base properties of IO_2F_3.

Engelbrecht et al.[2] have studied the fluoride ion acceptor properties of IO_2F_3 and have shown that with HF the acid $HOIOF_4$ is obtained and that with various metal fluorides, MF_n one obtains the salts MIO_2F_4. They have also interpreted the ^{19}F NMR spectrum of the adduct $(IO_2F_3{\cdot}IOF_3)_n$ in terms of the ionic structure $IOF_2^+IO_2F_4^-$. From the reaction of IO_2F_3 with SbF_5 they obtained a white crystalline solid of mp 102 °C. The molten compound had a ^{19}F NMR spectrum consisting of an A_2B_2 and an A_4 spectrum in both the F on Sb and the F on I regions. They interpreted this result in terms of a polymeric structure containing both cis and trans oxygen bridges between $-IO_2F_4-$ and $-SbF_4-$ units. On the basis of a Raman spectroscopic study, Aubke[3] and co-workers have come to a different conclusion concerning the structure of $(IO_2F_3{\cdot}SbF_5)_n$. They proposed that it retains a polymeric IO_2F_3 structure, whose nature was not specified exactly, with SbF_5 groups coordinated to the IO groups of the IO_2F_3 polymer.

In our own studies of the donor–acceptor properties of IO_2F_3 we have prepared the adducts of IO_2F_3 with AsF_5, SbF_5, NbF_5, TaF_5, IF_5, and IOF_3 and we have investigated their structures by means of ^{19}F NMR and Raman spectroscopy. We have also prepared KIO_2F_4 and the adduct $KIO_2F_4{\cdot}2IF_5$ and have studied both compounds in the solid state and in solution in acetonitrile and in iodine pentafluoride by NMR and Raman spectroscopy.

Results and Discussion.

$IO_2F_3{\cdot}SbF_5$. The reaction between IO_2F_3 and SbF_5 gave a viscous colorless liquid very similar to pure SbF_5. The solution crystallized over a period of several days to give a white crystalline solid (mp 97–105 °C). The ^{19}F NMR spectrum of the melt is shown in Figure 2 and the NMR parameters derived from the spectrum of this and the other adducts are given in Table I. The main peaks in the spectrum are an A_2B_2 multiplet and a single line A_4 in both the F on I(VII) and F on Sb(V) regions. The only reasonable explanation for the two sets of A_2B_2 multiplets is that the adduct contains oxygen-bridged *cis*-IO_2F_4 and *cis*-SbF_4 units, as was previously concluded by Engelbrecht et al.[2] The single lines in each region of the spectrum can be assigned to the trans units in the adduct, i.e., to A_4 spin systems. The greater relative intensity of the A_4 singlet in the F on Sb region than that in the F on I(VII) region indicates that there are more *trans*-SbF_4 units than *trans*-IO_2F_4 units. This interpretation of the NMR spectrum is supported by the observation that the axial–equatorial fluorine–fluorine coupling constant in a cis unit of the polymer was 231 Hz for the IO_2F_4 unit and 129 Hz for the SbF_4 unit. These values are close to the coupling constants of 212 Hz for $IO_2F_4^-$, 218 Hz for $HOIOF_4$,[4,5] 128 Hz for the SbF_4SO_3F polymer,[6] and 130 Hz for polymeric antimony pentafluoride.[7,8]

There are, in addition, weak peaks at ~−95, ~−75, −43, 93, 101, 122, and 125 ppm relative to $CFCl_3$. The peak at −43 ppm lies in the F on I(V) region of the spectrum and may be reasonably assigned to IOF_2^+ which has[9] a chemical shift of −46 ppm (with reference to $CFCl_3$) in a solution of SbF_5. The presence of IOF_2^+ is confirmed by the observation of a characteristic peak in the Raman spectrum at 970 cm^{-1}.[9] On slow sublimation of the $(IO_2F_4{\cdot}SbF_4)_n$ adduct the −43-ppm line and the other accompanying impurity bands were found to increase in intensity in the residue while the freshly melted sublimate contained only a trace of IOF_2^+ as indicated by the very low intensity of the −43-ppm and accompanying lines. It appears that $(IO_2F_4{\cdot}SbF_4)_n$ is thermally unstable in the molten state and slowly loses oxygen to give IOF_3 which ionizes to give IOF_2^+. The other weak impurity lines found together with the IOF_2^+ line in the NMR spectrum are presumably due to the anion accompanying the IOF_2^+.

$$IO_2F_4{\cdot}SbF_4 \rightarrow IOF_2^+SbF_6^- + {}^1/_2O_2 \quad (1)$$

The simplest assumption would be that the anion is SbF_6^-; however, this is not consistent with the number of observed peaks and presumably the SbF_6^- reacts with the $(IO_2F_4{\cdot}SbF_4)_n$ (eq 2), to give the complex anion $IO_2F_4{\cdot}Sb_2F_{10}^-$, isoelectronic

$$SbF_6^- + IO_2F_4{\cdot}SbF_4 \rightarrow IO_2F_4{\cdot}Sb_2F_{10}^- \quad (2)$$

with $Sb_3F_{16}^-$, which could plausibly give rise to the impurity lines in both the F on I(VII) and the F on Sb regions of the NMR spectrum. Prominent features of the weak peaks in the F on Sb region are a doublet and a broad line which at low temperature appear to further resolve into a doublet of doublets and a complex multiplet. This is consistent with the presence of an Sb_2F_{10} unit.[10]

The Raman spectra of all of the adducts exhibit a great number of lines and as a result a complete assignment is not possible. The iodine–oxygen stretching modes, however, are expected to have the highest frequencies and they can be assigned with confidence. A *cis*-IO_2F_4 unit with C_{2v} symmetry is expected to have Raman-active symmetric and antisymmetric IO_2 stretching modes whereas a *trans*-IO_2F_4 unit of D_{4h} symmetry is expected to have only a single Raman-active IO_2 stretching mode. The Raman spectrum of the solid $(IO_2F_4{\cdot}SbF_4)_n$ adduct is given in Figure 3B and Table II lists

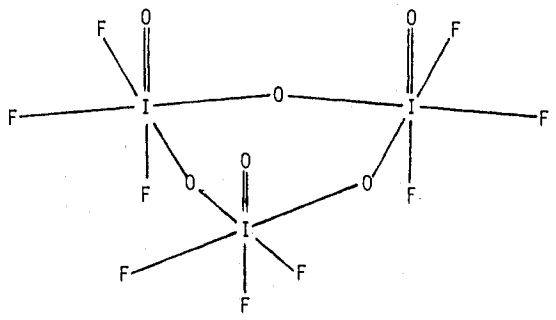

Figure 1. Structure of $(IO_2F_3)_3$.

the frequencies observed in the spectra of the solid and of the melt. Peaks were observed in the IO stretching region at 849 and 792 cm^{-1} which shifted to 880 cm^{-1} (polarized) and 815 cm^{-1} (depolarized), respectively, in the melt. Since the melt contains both *cis*- and *trans*-IO_2F_4 units, one would expect three IO stretches, of which two would be polarized. However, since only two bands are observed, one of which is polarized, we must conclude that the symmetric stretch of the *cis*- and *trans*-IO_2F_4 units are coincident and the band at 880 cm^{-1} is assigned to these modes, while the band at 815 cm^{-1} is assigned to the antisymmetric stretch of the cis isomer. It is difficult to assign the SbO stretching frequency due to the complexity of the spectrum but in the compounds $H_3O^+SbF_5OH^-$, $SbF_5 \cdot H_2O$, $SbF_5 \cdot SO_2$, and $Cs_2Sb_2F_{10}O$ the SbO stretching frequency occurs at 470,[11] 488 and 519,[12] and 467 cm^{-1},[13] respectively, and we, therefore, tentatively assign the depolarized peak at 463 cm^{-1} (481 cm^{-1} in the solid) to the SbO antisymmetric stretch and the polarized peak at 442 cm^{-1} (434 cm^{-1} in the solid) to the symmetric stretch of both *cis*- and *trans*-O_2SbF_4 units.

$IO_2F_3 \cdot AsF_5$. The reaction of IO_2F_3 with AsF_5 gave colorless crystals of the adduct which melted at about 40 °C. The ^{19}F NMR spectrum of the supercooled melt at 40 °C is shown in Figure 4 and the chemical shifts and coupling constants are listed in Table I. The spectrum consists of a multiplet and a very weak doublet in the fluorine on iodine(VII) region at low field and a single broad line in the fluorine on arsenic region at high field. Although the multiplet was not well resolved at 40 °C, at 10 °C it appeared to be an A_2B_2 spectrum with a single superimposed line. The A_2B_2 spectrum can be assigned to *cis*-IO_2F_4 units and the single line to the four equivalent fluorines of *trans*-IO_2F_4 units. The small doublet D, at −103 ppm, is attributed to the X_2 part of an AX_2 spectrum arising from a small amount of unreacted IO_2F_3. The two main resonances were found to have the same area in agreement with the formulation $(IO_2F_4 \cdot AsF_4)_n$. The coupling constant of 202 Hz for the *cis*-IO_2F_4 unit agrees well with the values found for the other $(IO_2F_4 \cdot MF_4)_n$ adducts described in this paper (Table I). On warming the complex above its melting point, dissociation occured as indicated by the increase in the intensity of the doublet D due to IO_2F_3. At 50 °C the F on I multiplet collapsed to a single line indicating a relatively rapid exchange of all of the fluorines of the *cis*- and *trans*-IO_2F_4 units at this temperature. The F on As resonance was a broad line at all temperatures between 10 and 50 °C presumably as a consequence of the almost complete collapse of the expected multiplet structure due to quadrupole relaxation of the arsenic nucleus.

The solid-state Raman spectrum of the adduct at −100 °C is shown in Figure 3A. There are three peaks in the I=O stretching region at 918, 846, and 832 cm^{-1} which are tentatively assigned to unreacted IO_2F_3 and the symmetric and antisymmetric stretches, respectively, of the *cis*-IO_2F_4 unit.

$(IO_2F_3 \cdot NbF_5)_n$ and $(IO_2F_3 \cdot TaF_5)_n$. The reactions of NbF_5 and TaF_5 with IO_2F_3 were carried out using a small excess

Table I. ^{19}F NMR Parameters of Various IO_2F_3 Adducts

Adduct	Temp, °C	Moiety	J_{F-F}, Hz	Chem shift,[a] ppm
$(IO_2F_4 \cdot AsF_4)_n$[d]	10			
		cis-IO_2F_4	202	A_2 −83.7; B_2 −68.4
		trans-IO_2F_4		A_4 −69.6
		cis-AsF_4–*trans*-AsF_4	n.o.[b]	43.4
$(IO_2F_4 \cdot SbF_4)_n$[d]	36			
		IO_2F_3	179	A n.o.; B_2 −103.0
		cis-IO_2F_4	231	A_2 −96.7; B_2 −76.5
		trans-IO_2F_4		A_4 −81.9
		cis-SbF_4	129	A_2 87.4; B_2 116.0
		trans-SbF_4		A_4 92.3
		IOF_2^+ counterion (see text)	87	101.2; 125.4
		IOF_2^+[c]		A_2 −42.9
$(IO_2F_4 \cdot NbF_4)_n$[d]	36			
		cis-IO_2F_4	222	A_2 −91.2; B_2 −65.3
		trans-IO_2F_4		A_4 −69.5
		cis-NbF_4–*trans*-NbF_4	n.o.	−219.8
$(IO_2F_4 \cdot TaF_4)_n$[d]	36			
		cis-IO_2F_4	215	A_2 −93.4; B_2 −67.6
		trans-IO_2F_4		A_4 −72.0
		cis-TaF_4	n.o.	A_2 −137.6
		trans-TaF_4		A_4 −140.0
$(IO_2F_4 \cdot IF_4)_n$ in excess IF_5	−10			
		cis-IO_2F_4	220	A_2 −99.5; B_2 −78.1
		trans-IO_2F_4		A_4 −82.3
		IF_4	n.o.	A_2' −33.0; B_2' −17.8
		IO_2F_3	188	A n.o.; B_2 −109.3
		IF_5	89	A'' −58.9; X_4 −9.7
$IO_2F_4 \cdot H$[e]	36			
		cis-IO_2F_4	21	A_2 −92.9; B_2 −68.8
		trans-IO_2F_4		A_4 −70.5
$IO_2F_4 \cdot IOF_2$	83			
		cis-IO_2F_4	214	A_2 −105.9; B_2 −77.8
		trans-IO_2F_4		A_4 −82.2
		IOF_2		A_2' −28.0
KIO_4 in IF_5	36			
		cis-$IO_2F_4^-$	202	A_2 −102.1; B_2 −68.5
		trans-$IO_2F_4^-$		A_4 −70.6
		IF_5	n.o.	A' −56.1; X_4 −9.9
$KIO_2F_4 \cdot 2IF_5$[f] in excess CH_3CN	36			
		trans-$IO_2F_4^-$		A_4 −62.0
		IF_5	76	A −48.1; X_4 −2.4

[a] Chemical shift with respect to external $CFCl_3$. [b] Not observed. [c] From IO_2F_3 photodecomposition or thermal decomposition

$$IO_2F_3 \xrightarrow{h\nu} IOF_3 + {}^1/_2O_2 \xrightarrow{SbF_5} IOF_2^+SbF_6^-$$

[d] Spectra recorded on molten adducts. [e] This work. [f] $KIO_2F_4 \cdot 2IF_5$ adduct dissolved in excess CH_3CN.

Table II. Raman Spectra of Some IO_2F_3 Adducts (cm^{-1})

$(IO_2F_4 \cdot NbF_4)_n$ Solid[a]	$(IO_2F_4 \cdot TaF_4)_n$ Solid[b]	$(IO_2F_4 \cdot SbF_4)_n$ Solid[b]	$(IO_2F_4 \cdot SbF_4)_n$ Melt	$(IO_2F_4 \cdot AsF_4)_n$ Solid[a]	$(IO_2F_4 \cdot IOF_2)_n$ Solid[b]	$(IO_2F_4 \cdot IF_4)$ soln in IF_5	Description of motion
	956 (1)		970 (1)				IO str of IOF_2^+
					927 (4)		IO str of IOF_2
					915 (69)		
913 (4)				918 (4)		915 sh	IO str of IO_2F_3
887 sh	889 sh						
879 (17)	879 (18)		880 (21) p				IO_2 sym str of IO_2F_4
868 (28)		849 (17)		846 (4)	804 (22)	896 (27)	
811 (26)	820 sh						
804 (38)	813 (16)	792 (5)	815 (5) dp	832 (7)	750 (9)	757 (6)	IO_2 antisym str of IO_2F_4
				761 (20)			
740 sh				745 (57)			
				736 (10)			
729 (92)		727 (17)	738 sh	726 (21)			
	715 sh			720 (36)			
	713 (100)	715 (100)					
701 (46)		705 (28)	708 (100) p		706 sh	703 sh	
693 (42)		695 (14)		698 (27)	694 (25)		
		691 (14)				687 (100)	
	689 (22)	687 (12)	685 sh				
		680 sh		680 (15)			
678 sh	675 (22)	677 (30)		673 (10)	673 (100)		
670 (28)							
	661 (23)	664 (58)	664 (77) p	666 (100)			
654 (100)	650 (22)						
647 (28)			647 sh	647 (57)	645 (31)		
	639 sh		636 (67) p		635 (16)	636 (55)	
629 (7)	629 sh	629 (67)	615 sh	620 (4)	629 sh		
					618 (22)		
					606 (31)	603 (66)	
						579 sh	
515 (2) vbr	490 (1) vbr	481 (3)	463 sh dp	508 (5)		467 sh	
452 (8)	458 (9)	434 (21)	442 (21) p	472 sh	549 (8)	447 (5)	
				461 (22)	538 sh		
436 (12)	431 (7)						
423 (11)					425 sh		
413 (17)	413				416 (2)		
				400 (6)	402 (1)		
384 (14)	385 (10)			392 (14)	380 (2)		
373 (9)	376 (7)	378 (8)	378 (9) dp	371 (8)	373 (2)	374 (24)	
366 (9)							
358 (9)	358 sh	351 (11)	349 (15) dp	351 (7)			
351 (13)	351 (12)						
				344 (6)	347 (3)	351 (8)	
					329 (3)		
				323 (16)	323 (3)		
289 (3)	285 (4)	296 (8)	289 (11)	298 (15)	289 (5)	314 (8)	
278 (4)	278 (2)	274 (7)	271 (11)	278 (4)			
261 sh	261 sh			269 (7)	261 (2)	268 (24)	
252 (20)	254 (21)	259 (18)		254 (4)	250 (1)	257 sh	
	241 sh		238 (7)	243 (3)			
237 (10)	235 sh	234 (7)			232 (1)		
221 (12)	226 (23)						
		197 (31)	195 (8)	206 (27)		206 (17)	
172 (25)	172 (13)	176 (26)	175 (13)	169 (3)	165 (2)		
165 sh	158 (13)			152 (23)	150 (2)		
	130 (5)			143 (6)		126 (20)	
				111 (7)	115 (3)		
				102 (6)			

[a] At −100 °C. [b] Room temperature.

of IO_2F_3. The adducts formed were microcrystalline solids with melting points of about 100 °C. The F on I(VII) region only of the NMR spectra of the supercooled melts at 94.1 MHz and 36 °C are shown in Figure 5. Both spectra exhibit the characteristic A_2B_2 and A_4 spectra of the *cis*- and *trans*-IO_2F_4 units, respectively. The F on Nb and F on Ta resonances consist of a single broad line, presumably due to the almost complete collapse of the expected multiplet by the quadrupole relaxation of the Nb and Ta nuclei. The F on Ta resonance also has a small shoulder to low field which may be due to the oxygen-bridged *trans*-TaF_4 units while the main broad resonance may be due to the cis units.

The Raman spectra of the two adducts are shown in Figure 3C and D. Both adducts show two sets of peaks in the IO region at ~878 and ~808 sm^{-1} for the NbF_5 adduct and ~884 and ~816 cm^{-1} for the TaF_5 adduct. In addition to these lines, which are readily assigned to the *cis*-IO_2F_4 units in the adducts, there is a peak at 913 cm^{-1} in the NbF_5 adduct which arises from excess IO_2F_3 and also a very weak peak at 956 cm^{-1} in the TaF_5 adduct which is assigned to the IO stretch of the IOF_2^+ cation. This impurity arises after heating and cooling the sample several times as in the case of the SbF_5 adduct. The lack of knowledge concerning the strength of the bridging bonds between IO_2F_4 and the MF_4 moiety and the

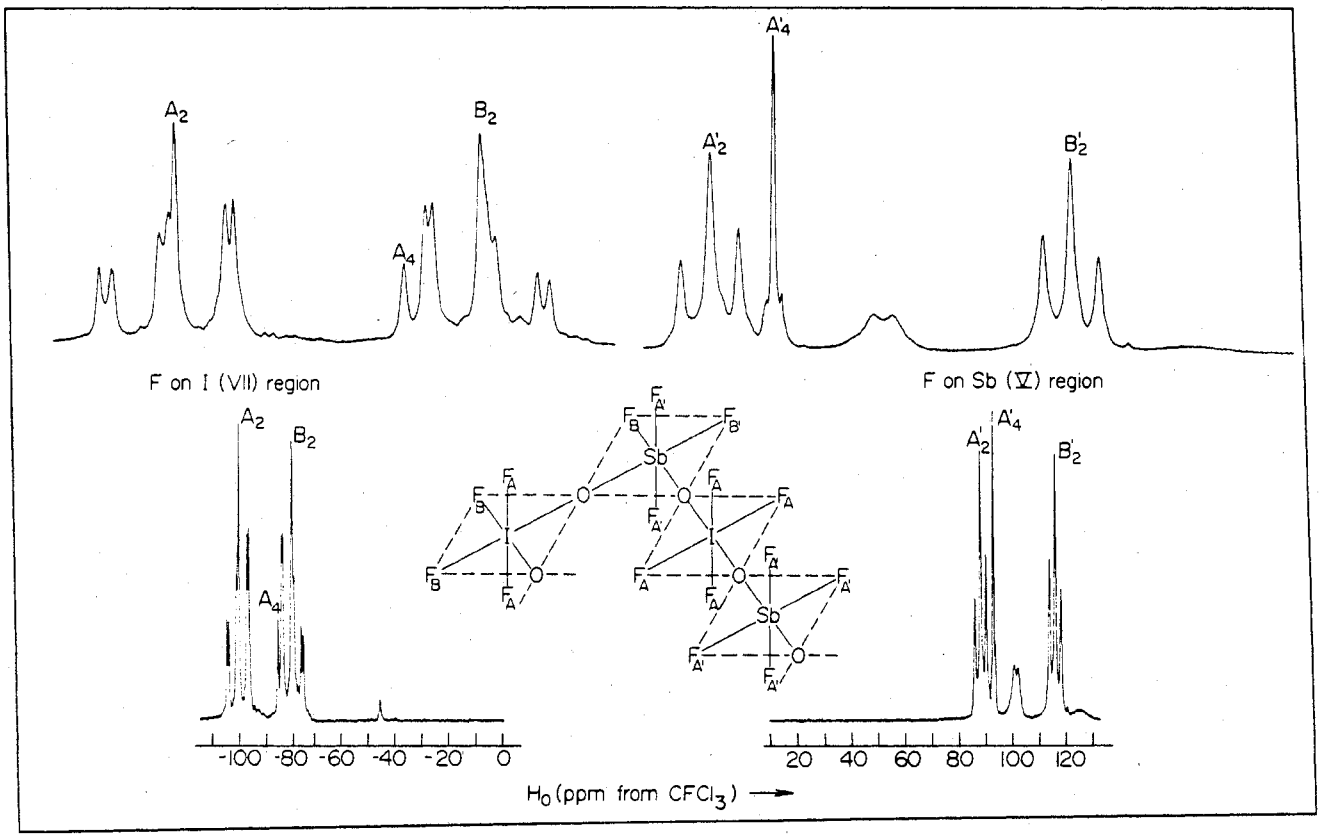

Figure 2. ^{19}F NMR spectrum of an equimolar mixture of IO_2F_3 and SbF_5 recorded as a supercooled melt at 36 °C. Inset: structural units (*cis*- and *trans*-IO_2F_4 and -O_2SbF_4) of the polymer.

Table III. Raman Spectra of KIO_2F_4, $KIO_2F_4 \cdot 2IF_5$, and a Solution of $KIO_2F_4 \cdot 2IF_5$ in Acetonitrile

ν, cm^{-1}				
$KIO_2F_4 \cdot 2IF_5$				
Solid	Soln	IF_5 In CH_3CN soln	KIO_2F_4 Solid	Assignment (D_{4h} $IO_2F_4^-$)
879 (0.5)	875 (3) p		879 (0.5)	$\nu_1(A_1)$ IO sym str (*cis*-$IO_2F_4^-$)
861 (1)			854 (0.5)	$\nu_3(A_{2u})$ IO asym str
			827 sh	
			821 sh	$\nu_1(A_{1g})$ IO sym str
808 (100)	816 (92) p		816 (100)	
694 (5)				
686 sh				
670 (73)	677 (100) p	678 (100) p		IF_5
635 sh				
611 (62)	586 (90) p	585 (90) p		
585 sh	[576 vbr dp][b]		581 (55)	$\nu_4(B_{2g})$ IF_4 out-of-phase str
572 (32)	[569 (40) dp][b]	569 (42) dp		IF_5
565 sh	567 (65) p		565 sh	$\nu_2(A_{1g})$ IF_4 in-phase str
395 (51)			395 (26)	
385 (19)	*a*		380 (40)	$\nu_5(E_g)$ OIF bend
		316 (6) p		
276 (5)	267 (8)	267 (9) dp		IF_5
			257 (9)	$\nu_6(B_{1g})$ IF_4 in-plane scissor

[a] Peaks obscured by strong acetonitrile peak. [b] Peaks in brackets obtained from $I_\perp$ spectrum (see text).

complexity of the Raman spectra precluded the assignment of the stretching modes associated with the bridge.

$(IO_2F_3 \cdot IF_5)_n$. The ^{19}F NMR spectrum of a solution containing IO_2F_3 in excess IF_5 was recorded at 10 °C, the lowest temperature at which all species remained in solution. The spectrum (Figure 6B) consists of the characteristic A_2B_2 and A_4 spectra in the F on I(VII) region associated with *cis*- and *trans*-IO_2F_4 units, together with X_2 doublet (E) of IO_2F_3, the A triplet being hidden by the B_2 triplet of the complex. The F on I(V) region exhibits the characteristic AX_4 spectrum of IF_5 (A″ and X_4) and two single broad lines (175 Hz at half-height) of equal intensity, at −33 and −17.8 ppm relative to $CFCl_3$, which are assigned to an incompletely resolved A_2B_2 spectrum associated with the IF_4 group. The adduct is not ionic since the NMR spectrum of a solution of IF_5 in excess SbF_5, in which IF_4^+ is formed,[14] shows a single broad peak at −36.3 ppm whereas the average chemical shift of the I(V) species in this adduct is −25.4 ppm. The observed spectrum, however, is consistent with a bridging IF_4 species with two sets of nonequivalent fluorines giving rise to an A_2B_2 spectrum, which together with two long bridging bonds and a lone pair completes an AX_6E stereochemistry around the iodine.[15] Since spin–spin coupling is not observed, we conclude that there is intermediate rate exchange between the fluorines in the IF_4

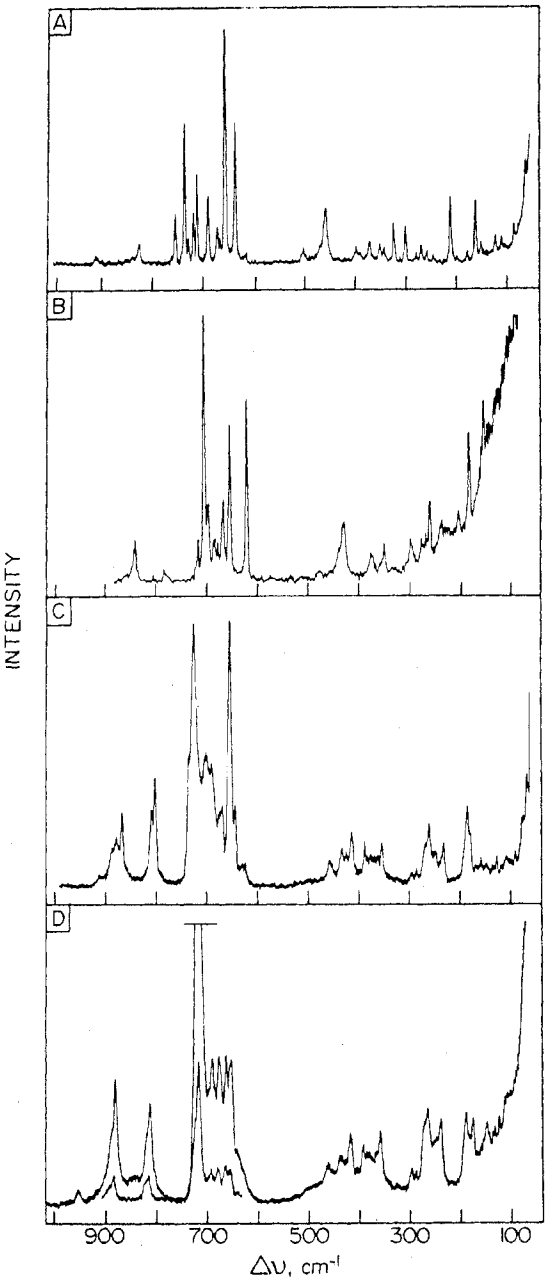

Figure 3. Solid-state Raman spectra: (A) $IO_2F_4 \cdot AsF_4$ adduct at −100 °C; (B) $IO_2F_4 \cdot SbF_4$ adduct; (C) $IO_2F_4 \cdot NbF_4$; (D) $IO_2F_4 \cdot TaF_4$ recorded at room temperature in a glass NMR sample tube.

group which is probably intramolecular.

The Raman spectrum of the solution at room temperature shows a broad peak at 896 cm^{-1} with a shoulder at 915 cm^{-1} and a peak at 757 cm^{-1}. The shoulder at 915 cm^{-1} is assigned to uncomplexed IO_2F_3. The peak at 896 cm^{-1} must be the I–O symmetric stretching frequency for both the *cis*- and *trans*-IO_2F_4 units, whereas the peak at 757 cm^{-1} is assigned to the asymmetric stretching frequency of the *cis*-IO_2F_4 units.

$(IO_2F_3 \cdot IOF_3)_n$. The ^{19}F NMR spectrum of the adduct formed from IOF_3 and IO_2F_3 was recorded on the supercooled melt at +83 °C (Figure 6A). The spectrum shows the characteristic A_2B_2 and A_4 patterns associated with *cis*- and *trans*-IO_2F_4 units I and II as well as a single line at −28.0 ppm relative to $CFCl_3$, which is assigned to the IOF_2 group in the complex. Engelbrecht and co-workers[2] assigned this peak to the IOF_2^+ cation but IOF_2^+ in SbF_5 solution has been found to have[9] a chemical shift of −46 ppm. Furthermore, Engelbrecht et al. used HSO_3F as an internal standard in obtaining the NMR spectrum of this adduct and we have shown elsewhere[9] that the IOF_2^+ cation reacts with HSO_3F to give a species of composition IOF_2SO_3F which has a fluorine on I(V) resonance at −26 ppm. Therefore, even if the $(IO_2F_3 \cdot IOF_3)_n$ complex was a salt of composition $IOF_2^+IO_2F_4^-$ as Engelbrecht claimed, it is doubtful that it would be stable in HSO_3F. The physical properties of the adduct are also in disagreement with its formulation as a salt since it has a relatively low melting point and it readily supercools. The ^{19}F NMR spectrum can be rationalized if we consider the IOF_2 group as a bridging pseudo-six-coordinate (AX_5E) I(V) species with C_s symmetry. There are alternative geometries for the IOF_2 group; however, according to the VSEPR theory,[15] the most stable geometry is likely to be the one shown, where the lone pair of electrons is trans to the doubly bonded oxygen. It must be supposed that structures I and II are in equilibrium in solution in order to account for the presence of both *cis*- and *trans*-IO_2F_4 groups.

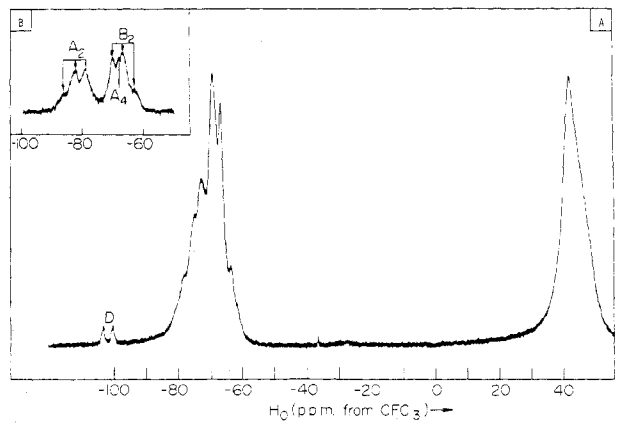

Figure 4. ^{19}F NMR spectrum of an equimolar mixture of IO_2F_3 and AsF_5 recorded at (A) 40 °C and (B) 10 °C. D is the B_2 doublet of dissociated IO_2F_3.

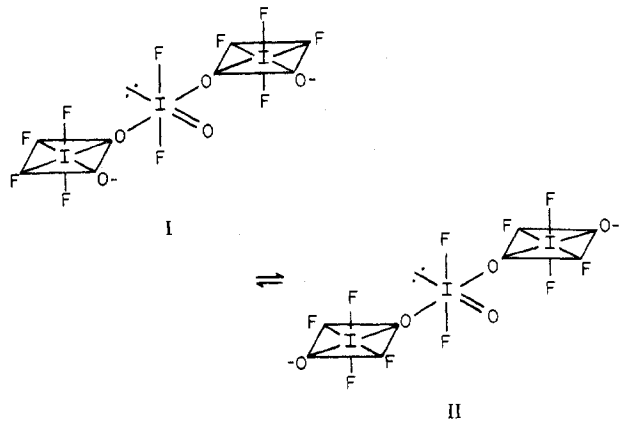

The observed Raman frequencies of the solid adduct are given in Table II. The complexity of the spectrum below 750 cm^{-1} restricts the assignments to the iodine(V) and iodine(VII) doubly bonded oxygen stretching modes. The I=O stretching frequency of crystalline IOF_3 is found at 891 cm^{-1} [9,16] (average of the frequencies of the five lines in the IO region arising from solid-state splittings). In the adduct, however, the vibrational mode associated with the I=O stretch of the IOF_2 moiety is assigned to the band at 915 cm^{-1} since this is consistent with the I(V) atom acquiring a small positive charge although not as large as that in IOF_2^+ where the IO stretching frequency occurs at 970 cm^{-1}.[9] The implication of this assignment is that the IO_2F_4 moiety is slightly anionic and hence the iodine-

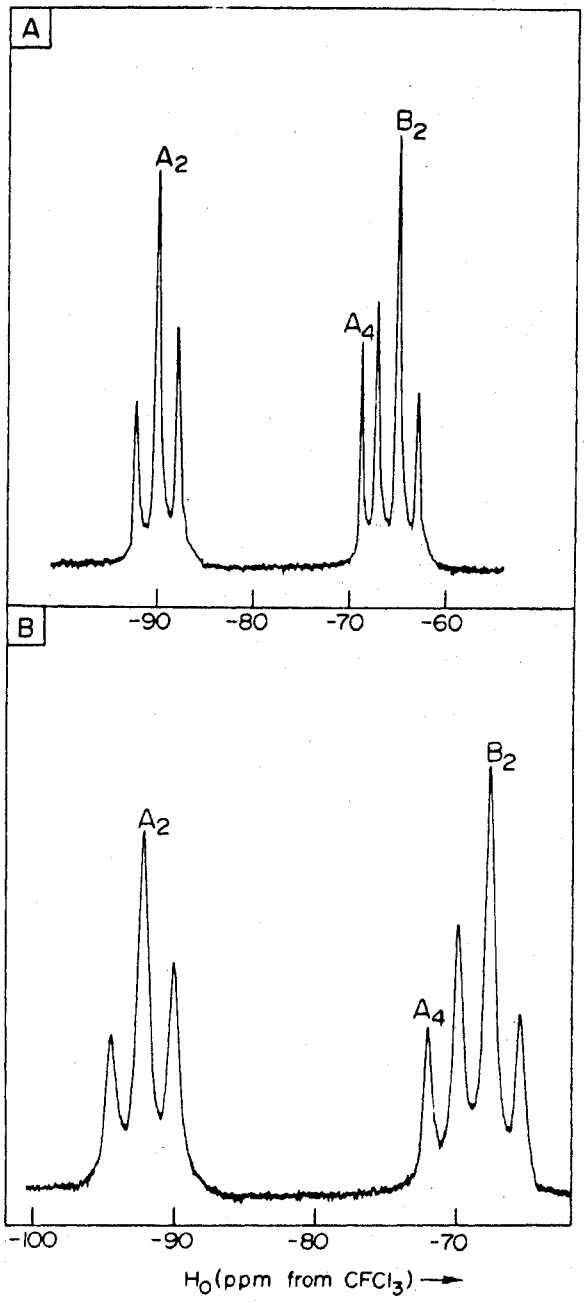

Figure 5. The 94.1-MHz ^{19}F NMR spectra of equimolar mixtures of (A) IO_2F_3 and NbF_5 and (B) IO_2F_3 and TaF_5 recorded as supercooled melts at 36 °C. Only the F on I(VII) region is shown.

(VII)–oxygen stretching frequencies are expected to be lower than the corresponding mode in IO_2F_3 which is found at 918 cm^{-1}.[2] The two peaks at 804 and 750 cm^{-1} are therefore assigned to the symmetric and antisymmetric $I^{VII}O_2$ stretching modes respectively in the IO_2F_4 units, by analogy with the other $(IO_2F_4 \cdot MF_4)_n$ adducts.

$KIO_4 \cdot IF_5$. Aynsley, Nichols, and Robinson[17] have reported that the reaction between KIO_4 and IF_5 gave a white solid of composition $KIO_4 \cdot IF_5$, after the removal of excess IF_5 at 120 °C under vacuum. There was no evidence on the structure of this material. We have obtained the room-temperature ^{19}F NMR spectrum of a solution of KIO_4 in IF_5 (Figure 7B). It showed the typical A_2B_2 and A_4 spectra in the F on I(VII) regions characteristic of *cis*- and *trans*-$IO_2F_4^-$, respectively. The expected well-resolved AX_4 pattern associated with the IF_5 solvent is partially collapsed and there is also a shoulder to low field of the X_4 resonance. The formation of $IO_2F_4^-$ and

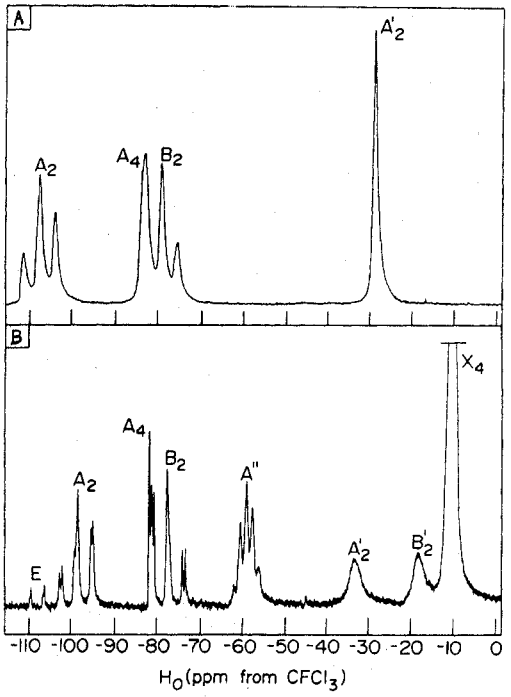

Figure 6. ^{19}F NMR spectra (58.3 MHz): (A) equimolar mixture of IO_2F_3 and IOF_3 recorded at +83 °C on a supercooled melt; (B) solution of IO_2F_3 in IF_5 at 10 °C (E is the B_2 doublet of unreacted IO_2F_3 and the resonances A″ and X_4 belong to the IF_5 solvent).

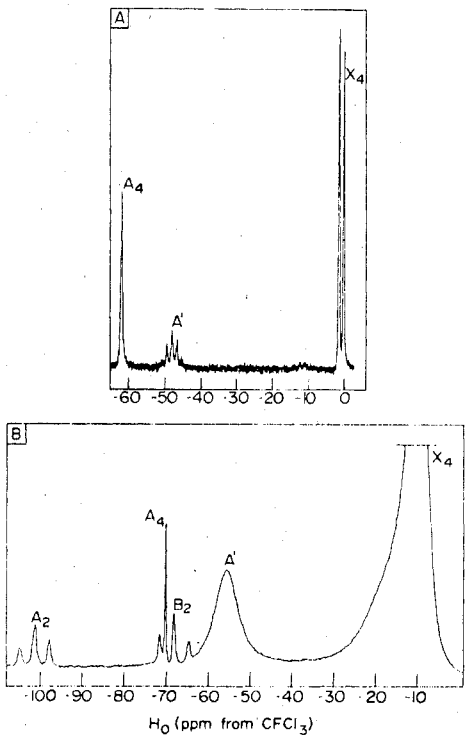

Figure 7. ^{19}F NMR spectra: (A) $KIO_2F_4 \cdot 2IF_5$ in acetonitrile at room temperature; (B) solution of KIO_4 in IF_5. The broad bands labeled A′ and X_4 belong to the IF_5 solvent.

the partial collapse of the AX_4 spectrum of IF_5 may be explained by the reactions

$$KIO_4 + IF_5 \rightarrow KIO_2F_4 \text{ (cis/trans)} + IO_2F \quad (3)$$

$$IO_2F + IF_5 \rightleftarrows 2IOF_3 \quad (4)$$

The shoulder of the X_4 resonance of IF_5 is attributable to an

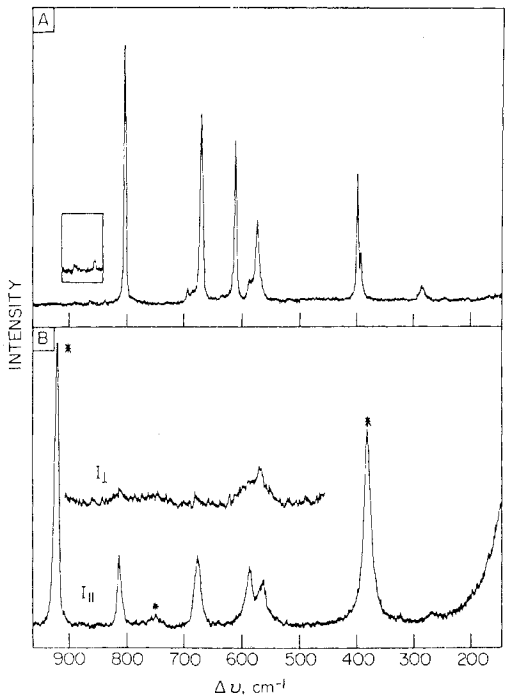

Figure 8. Raman spectra: (A) $KIO_2F_4 \cdot 2IF_5$ recorded in a glass NMR tube at room temperature (inset: 850–900-cm^{-1} region under higher gain); (B) $KIO_2F_4 \cdot 2IF_5$ in acetonitrile solution recorded in a glass NMR tube at room temperature (bands marked with an asterisk are acetonitrile bands).

equilibrium mixture of IO_2F and IOF_3 undergoing intermediate-rate fluorine exchange with IF_5 at room temperature. According to eq 3 and 4, if the solution of KIO_4 in IF_5 is pumped to dryness under vacuum, a solid containing a mixture of *cis*- and *trans*-KIO_2F_4, IO_2F, and IOF_3 is obtained. However, at 120 °C equilibrium 4 lies completely to the left[17] and the volatile IF_5 is removed leaving behind an equimolar mixture of KIO_2F_4 (cis/trans) and IO_2F. This mixture corresponds in composition to that of the $KIO_4 \cdot IF_5$ adduct reported by Aynsley and co-workers.[17]

$KIO_2F_4 \cdot 2IF_5$. On cooling of the solution of KIO_4 in IF_5, colorless crystals precipitated out. The composition of the crystals was found by elemental analysis to be $KIO_2F_4 \cdot 2IF_5$. The formation of this complex is consistent with the tendency of the isoelectronic salts MIF_6 to form $MIF_6 \cdot 2IF_5$ adducts.[18] The ^{19}F NMR spectrum of a solution of this material in acetonitrile, at room temperature (Figure 7A), showed the expected AX_4 pattern of IF_5 in addition to a singlet at −62 ppm. The area of this singlet relative to the quintet resonance of IF_5 indicated that it corresponds to four fluorines and this peak can, therefore, be assigned to *trans*-$IO_2F_4^-$. The chemical shift of this species in IF_5 is, however, −70.6 ppm and the difference from that in acetronitrile may be attributed, in part, to a solvent effect and also to slow exchange between *cis*- and *trans*-$IO_2F_4^-$ in IF_5 solution.

The Raman spectrum of $KIO_2F_4 \cdot 2IF_5$ is relatively simple and is essentially a composite of that of KIO_2F_4 and IF_5. It is interesting to note, however, that the IF_5 lines are sharper and slightly shifted from those in liquid IF_5 where association is assumed to occur.[19,20] The IF_5 can be removed from the solid adduct under vacuum at 90 °C or by dissolving it in acetonitrile and pumping off the solvent together with the IF_5. Under high gain two very small peaks (<1%) are observed in all of the solid-state spectra of KIO_2F_4 (Figure 8 and Table III) at 854 and 879 cm^{-1}. We assign the 854-cm^{-1} band to the antisymmetric IO_2 stretching mode of the trans isomer; this mode is Raman inactive but is presumably weakly allowed in the solid state due to a lowering of the site symmetry. The polarized band at 875 cm^{-1} (879 cm^{-1} in the solid) is assigned to the IO symmetric stretching mode of the cis isomer which is probably produced by a small degree of isomerization. The Raman spectra of KIO_2F_4 and $KIO_2F_4 \cdot 2IF_5$ both show that the $IO_2F_4^-$ in these compounds is the trans isomer of D_{4h} symmetry. Such an ion should have ten fundamental modes with symmetry designations $2A_{1g} + B_{1g} + B_{2g} + E_g + 3E_u + 2A_{2u}$. The A_{1g}, B_{1g}, B_{2g}, and E_g modes are Raman active only and therefore a total of five Raman lines are expected for this ion. In the solid-state spectrum of the *trans*-$IO_2F_4^-$ ion nine bands were observed but some of the lines are clearly due to solid-state effects. We assign the polarized solution band at 816 cm^{-1}, which had two shoulders at 821 and 827 cm^{-1} in the spectrum of the solid, to the IO_2 symmetric stretching frequency. Similarly the polarized peak at 567 cm^{-1}, which was observed as a shoulder at 565 cm^{-1} in the spectrum of the solid, is assigned to $\nu_2(A_{1g})$, the IF_4 in-phase stretching mode. In IOF_5[21,22] the corresponding mode, which is expected to have a higher frequency, was found at 640 cm^{-1}, whereas the out-of-phase stretch was found at 647 cm^{-1}. In IF_5[19,20] these modes occur at 593 and 575 cm^{-1} and we therefore assign the broad band at 576 cm^{-1} in acetonitrile solution and at 581 cm^{-1} in the solid to $\nu_4(B_{2g})$. The 576- and 569-cm^{-1} bands were completely obscured in the normal $I_\parallel$ spectrum of the solution by the intense peaks at 586 and 567 cm^{-1}. However, as these peaks are strongly polarized, their intensities were greatly reduced in the $I_\perp$ spectrum and this allowed the observation of the 576- and 569-cm^{-1} bands. The doubly degenerate vibration $\nu_5(E_g)$ is assigned to the two bands at 395 and 380 cm^{-1} by analogy with the corresponding bands in IOF_5 and IF_5 which are found at 375 and 374 cm^{-1}, respectively. The IF_4 in-plane scissor $\nu_6(B_{1g})$ is assigned to the band at 257 cm^{-1} in the solid-state spectrum. The ^{19}F NMR spectrum reported in Figure 7B shows that in IF_5 as a solvent, the *cis*-$IO_2F_4^- \rightleftarrows$ *trans*-$IO_2F_4^-$ equilibrium favors the cis form. Moreover, Carter et al.[3] have concluded that the direct reaction of CsF with IO_2F_3 produces *cis*-$IO_2F_4^-$. However, when $IO_2F_4^-$ is crystallized with two molecules of IF_5, the trans form is favored. This may be due to packing considerations in the solid if there is a weak interaction between basic O atoms of $IO_2F_4^-$ and the IF_5 molecules. This situation is analogous to that in $Sb_3F_{16}^-$ where the cis form is present in solution,[8] but the trans form has been found in the solid.[23] When crystalline $KIO_2F_4 \cdot 2IF_5$ was dissolved in CH_3CN and the volatiles were removed under vacuum, *trans*-KIO_2F_4 was isolated. The work of Engelbrecht et al.[4,5] has shown that isomerization of the cis and trans forms of $HOIOF_4$ readily occurs in solvents in which F^- transfer is possible. However, in CH_3CN the isomerization of $IO_2F_4^-$ is much slower and allows the trans form to be isolated from the $KIO_2F_4 \cdot 2IF_5$ complex.

Conclusions

All of the adducts of IO_2F_3 and Lewis acid pentafluorides that we have studied have polymeric structures containing IO_2F_4 groups alternating with O_2MF_4 groups. In solution and in the molten state it is clear from the NMR spectra that both the O_2MF_4 and the IO_2F_4 units exhibit cis–trans isomerism, with the cis isomers being favored. Figure 9 shows a relationship between IO bond order and the mean IO stretching frequency for some iodine(VII)–oxo compounds which gives IO bond orders in the $(IO_2F_3 \cdot MF_5)_n$ adducts in the range 1.5–1.7. Presumably the structure of these adducts can be approximately represented by a variety of resonance structures such as III–VI. These are consistent with the double-bond character of the IO bonds and they suggest also that the MO bond order is less than unity. This conclusion formed the basis of our assignment for the Sb–O stretching frequencies in the $(IO_2F_4 \cdot SbF_4)_n$ adduct.

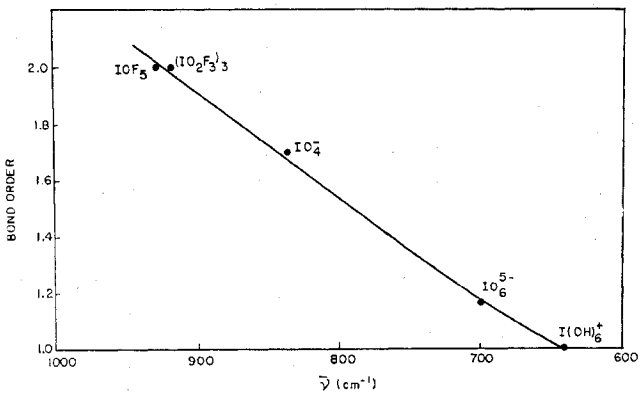

Figure 9. IO bond order–stretching frequency relationship.

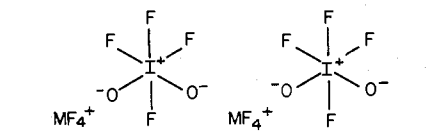

III

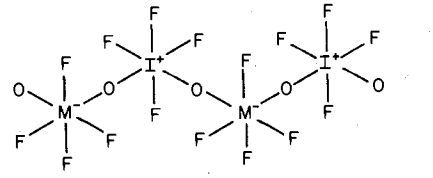

IV

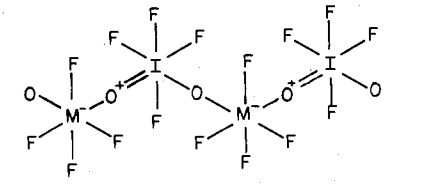

V

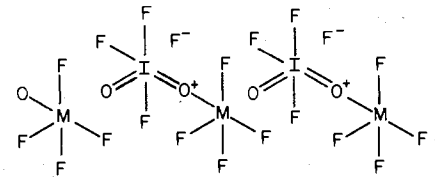

VI

Although SbF_5 is an exceptionally strong Lewis acid that can extract a fluoride ion from many other fluorides MF_n to give ionic compounds such as $MF_{n-1}^+SbF_6^-$ and $MF_{n-1}^+Sb_2F_{11}^-$, it appears that it is unable to extract a fluoride ion from IO_2F_3 according to the equation

$$IO_2F_3 + SbF_5 \rightarrow IO_2F_2^+ + SbF_6^-$$

Indeed it seems that IO_2F_3 can extract a fluoride ligand from SbF_5 according to the equation

$$IO_2F_3 + SbF_5 \rightarrow IO_2F_4 \cdot SbF_4$$

At first sight one might be tempted to speculate that IO_2F_3 is a stronger Lewis acid than SbF_5. However, such a comparison of acidities is not too meaningful without a detailed consideration of the mechanism of the reaction. Indeed it seems likely that the first step of the reaction is the formation of an oxygen-bridged adduct VII analogous to that formed between IOF_5 and SbF_5.[9] In this adduct the antimony would have a negative charge and the iodine a positive charge by virtue of a contribution from the structure VIII. These charges would facilitate the transfer of F^- from Sb to iodine giving a

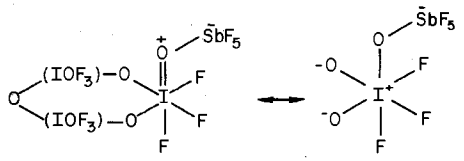

VII VIII

seven-coordinate intermediate IX. If this were followed by

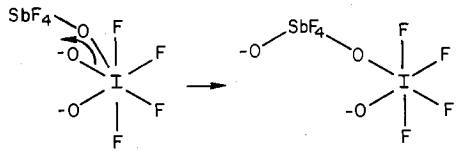

IX X

I–O bond cleavage and Sb–O bond formation, a polymeric chain would be obtained with six-coordinate antimony and iodine species in alternate positions as in X.

Experimental Section

Iodine Dioxide Trifluoride. IO_2F_3 was prepared by the method of Engelbrecht and Peterfy[4,5] by the addition of oleum to a solution of $HOIOF_4$ in HSO_3F and subliming IO_2F_3 out of solution. Care was taken to add 65% oleum very slowly to the reaction mixture; otherwise decomposition with evolution of oxygen occurred.

Antimony Pentafluoride. SbF_5 was obtained from Ozark Mahoning Co. and was purified by double distillation at atmospheric pressure in an all-glass apparatus.

Arsenic Pentafluoride. AsF_5 was obtained from the Ozark Mahoning Co. and was used directly.

Niobium and Tantalum Pentafluorides. NbF_5 and TaF_5 were obtained from the Ozark Mahoning Co. and were purified by vacuum sublimation in an all-glass apparatus.

Iodine Pentafluoride. IF_5 was obtained from the Matheson Co. and was purified by bubbling fluorine through the impure material until the solution was clear, followed by distillation from NaF to remove traces of HF.

Iodine Oxide Trifluoride. IOF_3 was made by the method of Aynsley, Nichols, and Robinson.[17]

Potassium Periodiate. KIO_4 was obtained from the Fisher Scientific Co. and dried at 180 °C in vacuo.

Preparation of the Adducts. All of the adducts were made in clear Pyrex glass NMR tubes fitted with Teflon valves. All materials were handled in a drybox with the exception of AsF_5 which was vacuum-distilled using a calibrated vacuum line. The SbF_5 and AsF_5 adducts with IO_2F_3 were made up to, as close as possible, a 1:1 stoichiometry whereas the NbF_5, TaF_5, and IOF_3 adducts were made using excess IO_2F_3, and the remaining unreacted IO_2F_3 was removed by sublimation.

The adduct of KIO_2F_4 with IF_5 ($KIO_2F_4 \cdot 2IF_5$) was made by dissolving KIO_4 in boiling IF_5 and allowing the solution to cool to room temperature at which point colorless crystals separated from solution. The solution was filtered and recrystallization was done from fresh IF_5; the solution was filtered again, and the remaining IF_5 was pumped away at room temperature under reduced pressure. The composition of the solid was determined by elemental analysis to be $KIO_2F_4 \cdot 2IF_5$. Anal. Calcd for $KIO_2F_4 \cdot 2IF_5$: K, 5.44; I, 53.03; F, 37.05. Found: K, 5.32; I, 51.71; F, 36.43. The adduct of composition $KIO_4 \cdot IF_5$ first obtained by Aynsley et al.[17] can be prepared if the solution of KIO_4 in IF_5 is pumped to dryness without first filtering the crystals.

Raman and NMR instrumentation have been described elsewhere.[12]

Elemental analysis was performed by Alfred Bernhardt Co., Mülheim, West Germany.

Acknowledgment. We thank the National Research Council of Canada for financial support of this work.

Registry No. $IO_2F_4 \cdot AsF_4$, 62139-92-8; $IO_2F_4 \cdot SbF_4$, 62139-93-9; $IO_2F_4 \cdot NbF_4$, 62139-62-2; $IO_2F_4 \cdot TaF_4$, 62139-63-3; $IO_2F_4 \cdot IF_4$, 62139-64-4; $IO_2F_4 \cdot H$, 62139-65-5; $IO_2F_4 \cdot IOF_2$, 53702-39-9; KIO_4, 7790-21-8; $KIO_2F_4 \cdot 2IF_5$, 62154-42-1; KIO_2F_4, 62154-40-9; IF_5, 7783-66-6.

References and Notes

(1) R. J. Gillespie and J. P. Krasznai, *Inorg. Chem.*, **15**, 1251 (1976).
(2) A. Engelbrecht, O. Mayr, G. Ziller, and E. Schandara, *Monatsh. Chem.*, **105**, 796 (1974).
(3) H. A. Carter, J. M. Ruddick, J. R. Sams, and F. Aubke, *Inorg. Nucl. Chem. Lett.*, **11**, 29 (1975).
(4) A. Engelbrecht and P. Peterfy, *Angew. Chem.*, **81**, 753 (1969).
(5) A. Engelbrecht, P. Peterfy and E. Schandara, *Z. Anorg. Allg. Chem.*, **384**, 202 (1971).
(6) R. J. Gillespie and R. A. Rothenbury, *Can. J. Chem.*, **42**, 416 (1964).
(7) C. J. Hoffman, B. E. Holder, and W. L. Jolly, *J. Phys. Chem.*, **62**, 364 (1958).
(8) J. Bacon, P. A. W. Dean, and R. J. Gillespie, *Can. J. Chem.*, **48**, 3414 (1970).
(9) J. P. Krasznai and R. J. Gillespie, to be submitted for publication.
(10) P. A. W. Dean and R. J. Gillespie, *J. Am. Chem. Soc.*, **91**, 7260 (1969).
(11) L. Kolditz and K. Bauer, *Z. Chem.*, **3**, 312 (1963).
(12) R. J. Gillespie and G. J. Schrobilgen, *Inorg. Chem.*, **15**, 22 (1976).
(13) W. Haase, *Chem. Ber.*, **106**, 41 (1973).
(14) K. O. Christe and W. Sawodny, *Inorg. Chem.*, **12**, 2879 (1973).
(15) R. J. Gillespie, "Molecular Geometry", Van Nostrand-Reinhold London, 1972, p 74.
(16) H. A. Carter and F. Aubke, *Inorg. Chem.*, **10**, 2296 (1971).
(17) E. Aynsley, E. Nichols, and P. L. Robinson, *J. Chem. Soc.*, 623 (1953).
(18) K. O. Christe, *Inorg. Chem.*, **11**, 1215 (1972).
(19) G. M. Begun, W. H. Fletcher, and D. F. Smith, *J. Chem. Phys.*, **42**, 2236 (1965).
(20) H. Selig and H. Holtzman, *Isr. J. Chem.*, **7**, 417 (1969).
(21) D. F. Smith and G. M. Begun, *J. Chem. Phys.*, **43**, 2001 (1965).
(22) J. H. Holloway, H. Selig, and H. H. Claassen, *J. Chem. Phys.*, **54**, 4305 (1971).
(23) A. J. Edwards, G. R. Jones, and R. J. Sills, *J. Chem. Soc., Chem. Commun.*, 1527 (1968).

Contribution from the Chemistry Department,
University of Manchester, Manchester M13 9PL, United Kingdom

Low-Energy Photoelectron Spectroscopy of Solids. Electronic Structure of the Cyanide, Nitrite, and Nitrate Ions

M. CONSIDINE, J. A. CONNOR,* and I. H. HILLIER

Received June 8, 1976 AIC60424B

An apparatus for recording the He I and He II photoelectron spectra of materials in the form of evaporated films is described. The photoelectron spectra of cyanide, nitrite, and nitrate ions are presented, and the ionization potentials and photoionization cross sections are interpreted using ab initio molecular orbital calculations. It is shown that low-energy spectra are much more useful than high-energy (ESCA) spectra for obtaining information on the valence electronic structure of solids. A different assignment of the ESCA spectrum of cyanide ion is proposed, and certain ambiguities in the assignment of the ESCA spectra of nitrate and nitrite ions are resolved.

1. Introduction

The use of photoelectron spectroscopy to study molecular electronic structure is now well established. The application of this technique to the study of solid materials has been undertaken predominantly using high-energy photons (ESCA or XPS), which because of their greater energy permit the measurement of core electron binding energies. Moreover, the availability of efficient vacuum locks, resulting from a less stringent vacuum requirement, allows greater ease in the preparation and introduction of samples. However, the use of ESCA to study the valence electron photoionization of solid samples is limited by the inherent line width of the ionizing radiation (ca. 1 eV) and the relatively low ionization cross section of the valence electrons compared with the more tightly bound core electrons.

The use of low-energy photons (ultraviolet photoelectron spectroscopy, UPS) for the study of solids is hampered by a stringent requirement for ultrahigh-vacuum facilities and the problems of producing high intensities of helium(II) in a windowless source under these conditions. If these difficulties can be overcome the potential benefits of UPS in the study of valence electron photoionization are manifold because of the high cross sections and the improvement in resolution arising from the narrow line width of the radiation (less than 10 meV).

Previous studies of the electronic structure of ionic solids using ESCA have shown that the lack of resolution and intensity do not usually allow an identification of all the low-lying ionized states of the molecules. In order to gain a better understanding of the electronic structure of relatively involatile solids, we have developed a photoelectron spectrometer to measure their ionization potentials using He I and He II ionizing radiation. In this paper we describe the application of the technique to the study of the cyanide, nitrite, and nitrate anions.

2. Experimental Section

a. The Spectrometer. The spectrometer chamber is of stainless steel construction with all-metal seals. The chamber is pumped by a 4-in. oil diffusion pump (Edwards E04) which is backed by a rotary pump (Edwards ED50) and is topped by a water-cooled baffle and a liquid nitrogen cold trap. The whole spectrometer chamber can be baked out at temperatures up to 200 °C. Typical pressures attained after baking the chamber for 12 h (overnight) at 160 °C are in the range (1–2) $\times 10^{-9}$ Torr, although the ultimate pressure achievable is 2×10^{-10} Torr.

The light source is a differentially pumped windowless 5-kV dc helium discharge lamp similar to the type (WG-031) commonly employed on the AEI ES200B spectrometer. He II intensities ($h\nu$ = 40.8 eV), obtained by reducing the helium pressure in the lamp, are usually 2–15% of the He I intensities ($h\nu$ = 21.2 eV). With the lamp operating in the He II mode the pressure in the main chamber rises to 3×10^{-9} Torr; in the He I mode the pressure in the chamber is in the range 5×10^{-9}–10^{-8} Torr. The spectrometer chamber is additionally equipped with an argon ion gun (Vacuum Generators AG2) and a quadrupole mass spectrometer (Vacuum Generators Q7). The sample probe is a stainless steel plate isolated from earth and mounted on a rotary motion drive (Vacuum Generators RD3) to which an angle-measuring device has been attached. Included between the rotary drive and the spectrometer chamber is an adjustable bellows which permits alignment of the sample with the light source and the analyzer slit.

The electron energy analyzer is a 5-cm mean radius electrostatic hemispherical analyzer (AEI). Photoelectrons from the sample, after passing through a 1-mm slit, are focused so that the slit is imaged at the analyzer entrance plane. The analyzer is held at a fixed transmission energy and energy analysis is performed by preretardation (or preacceleration) of the electrons before entering the analyzer. This is achieved by floating the hemispheres up on the scanning voltage.